Journal of Medical Virology

WILEY

JOURNAL OF MEDICAL VIROLOGY

RESEARCH ARTICLE

Oral *Neisseria gonorrhoeae* Promotes KSHV Lytic Replication

Shu Feng[1,2] | Wen Fu[1] | Shutong Li[1] | Wayne Yeh[1] | Rosemary She[3,4] | Charles Brenner[2] | Casey Chen[1] | Pinghui Feng[1]

[1]Section of Infection and Immunity, Herman Ostrow School of Dentistry, University of Southern California, Los Angeles, California, USA | [2]Department of Diabetes and Cancer Metabolism, Beckman Research Institute of City of Hope, Duarte, California, USA | [3]Norris Comprehensive Cancer Center, University of Southern California, Los Angeles, California, USA | [4]Department of Pathology, Duarte, California, USA

Correspondence: Shu Feng (sfeng@coh.org) | Pinghui Feng (pinghuif@usc.edu)

Received: 2 January 2025 | **Revised:** 13 February 2025 | **Accepted:** 8 March 2025

Keywords: bacteria-virus interaction | glycolysis | KSHV lytic replication | *Neisseria gonorrhoeae* | purine metabolism and pyrimidine metabolism | RTA

ABSTRACT

The human oral cavity contains highly diverse microbes, including bacteria, fungi, and viruses. Human herpesviruses are ubiquitous pathogens, and the oral cavity is conducive to the replication, dissemination, and pathogenesis of human herpesviruses. Herpesviruses are generally pathogenic in immunodeficient individuals, such as AIDS patients and organ transplant recipients. Kaposi's sarcoma-associated herpesvirus (KSHV) is the etiological agent of Kaposi's sarcoma and two types of rare lymphoma, that is, primary effusion lymphoma and multicentric Castleman's disease. Mounting evidence indicates that KSHV viral load positively correlates with ongoing bacterial infection in the oral cavity, suggesting that bacteria potentially stimulate KSHV replication. However, the mechanism by which oral bacteria may promote KSHV lytic replication is poorly understood. In this study, we performed DNA sequencing and 16S ribosomal RNA analysis of saliva samples of AIDS-KS patients. A correlation analysis identified a panel of oral residential bacteria and uncommon ones that paralleled with KSHV viral load. Performing functional assays, we discovered that the sexually transmitted *Neisseria gonorrhoeae* (*N.g.*) significantly increased KSHV lytic replication. Increased KSHV lytic replication was evidenced by elevated levels of mRNA and proteins of viral lytic genes. *N.g.* stimulation increases the expression of RTA that drives viral lytic replication. Metabolomic analysis reveals the synergistic effect of KSHV and *N.g.* on cellular metabolism, including the glycolysis and purine and pyrimidine synthesis, that likely underpins the elevated KSHV lytic replication. Findings from our study shed light on the molecular detail of bacteria–virus interaction in the oral cavity and provide references to develop an innovative strategy to treat diseases associated with KSHV.

1 | Introduction

The human oral microbiome contains highly diverse microbial communities, including bacteria, fungi, and viruses, which are the primary source of infectious agents. Human herpesviruses are ubiquitous pathogens, and the oral cavity is conducive to the replication, dissemination, and pathogenesis of human herpesviruses. Kaposi's sarcoma-associated herpesvirus (KSHV), also known as human herpesvirus 8, belonging to Gammaherpesvirinae subfamily, is the infectious agent of Kaposi's sarcoma (KS) [1], which is the most common AIDS-associated cancer worldwide [2]. KSHV infection tends to be latent in B cells but can switch to the lytic cycle triggered by host responses and various environmental factors, such as epigenetic modifications (e.g., demethylation), oxidative stress, and bacterial infection [3–7]. KSHV lytic replication is an integral component of KSHV-associated tumorigenesis. The oral cavity is the primary route of KSHV transmission among contagious individuals, and it is the site where KSHV reactivates in the oral epithelium and spreads to other cell types [8–10]. The roles of

oral bacteria in KSHV infection and reactivation have been increasingly appreciated. For example, *Pseudomonas aeruginosa* increased inflammatory cytokines and promoted the proliferation of KSHV-infected cells by LPS and flagellin [11]. Short-chain fatty acids (SCFAs), secreted by *Porphyromonas gingivalis* (*P.g.*) and *Fusobacterium nucleatum*, activated replication and transcription activator (RTA) for KSHV lytic replication in BCBL1 cells via inhibiting histone deacetylases, EZH2, and SUV39H1 [12]. These findings unveil the synergistic role of oral bacteria in KSHV pathogenesis and tumorigenesis.

Prompted by previous observation that KSHV load positively correlated with ongoing bacterial replication, we performed a metagenomic analysis of KS-positive AIDS patient saliva samples and identified a short list of bacteria that positively correlated with KSHV infection. Functional assays for KSHV lytic replication pinpointed *Neisseria gonorrhoeae* (*N.g.*) as a stimulator of KSHV replication. *N.g.* is the causative agent of gonorrhea, one of the most prominent sexually transmitted diseases worldwide [13]. In the United States, the prevalence of *N.g.* infection is increasing yearly, and it became the second most common notifiable sexually transmitted infection in 2021. In addition, oral sex, kissing, and saliva exchange can introduce *N.g.* to the oral cavity and cause typical oral gonorrhea [13, 14]. Oropharyngeal gonorrhea is generally asymptomatic, but the role of *N.g.* contributing to other oral infections and diseases is yet to be understood. Here, we report that *N.g.* in the saliva samples of KS patients can stimulate KSHV lytic replication. Interestingly, KSHV and *N.g.* synergistically reprogram cellular metabolism, particularly that of the glycolysis and nucleotide synthesis, to fuel viral lytic gene expression. Findings from this study advance our understanding of bacteria–virus interaction and cross-kingdom interaction in diseases associated with viral infections.

2 | Results

2.1 | *N.g.* Promotes KSHV Lytic Replication

KSHV was initially identified and isolated from AIDS patients [1]. Research on the association of AIDS and KS development primarily focuses on how HIV promotes KSHV replication and vice versa [15, 16]. In addition, KSHV transmission is not solely mediated by sexual contact, but also via saliva, transfusion, and transplant [17]. Human saliva contains diverse microorganisms, including bacteria, viruses, and fungi, constituting a complex system for interkingdom microbial interactions. To understand the possible roles of bacteria in KSHV pathogenesis, we first sequenced six saliva samples collected from AIDS-KS patients (Figure S1A), analyzed bacterial 16S ribosomal DNA, and constructed a list of oral bacterial pathogens that are more abundant in patient samples compared with those from healthy controls (Figure 1A and Table S1). KSHV load was confirmed by qRT-PCR using primers specific for the poly adenylated nuclear RNA (PAN) gene (Figure S1B,C). Although the genome copy number of KSHV varies among these six patients, they shared a similar spectrum of bacteria, such as *Aggregatibacter actinomycetemcomitans* (*A.a.*), *N.g.*, *Streptococcus mitis* (*S.m.*), *Streptococcus pneumoniae* (*S.p.*), and *P.g.* (Figures 1B and S2). Using KSHV load and bacteria genome frequency, we built a list of bacteria that positively correlate with KSHV genome copy number (Figure 1C). To identify which bacteria promote KSHV lytic replication, we performed a functional assay in which RGB-BAC16 KSHV replication was monitored in HOK cells with individual bacterium added. Human oral keratinocyte (HOK) is one of the few human cell lines that support KSHV lytic replication after de novo infection, although KSHV lytic replication is limited [18]. We first infected HOK cells with RGB KSHV at MOI = 30 for 6 h followed by bacterial infection with OD = 1.0 for 12 h and removed bacteria by rinsing with fresh medium. Strikingly, *N.g.* elevated KSHV lytic replication as indicated by GFP expression, by approximately twofold (Figure 1D,E). We next extended bacterial infection time to 18 h (Figure 1F) and observed more pronounced stimulation as indicated by GFP expression in all three coinfection groups with distinct *N.g.* strains, including F62, MS11, and FA1090 (Figure 1G). To further confirm the elevated KSHV lytic replication, GFP expression and viral titers in the medium were quantified at 72, 96, and 120 h.p.i. Indeed, *N.g.* infection elevated GFP expression as indicated by fluorescence image and increased infectious KSHV virions in the medium by ~10-fold (Figures 2A,B and S3A). Furthermore, *N.g.* stimulated KSHV lytic replication in a dose-dependent manner as indicated by GFP expression (Figure 2C).

To explore whether *N.g.* facilitates KSHV reactivation, HOK cells were first infected with rKSHV.219 at MOI = 5 or 10, followed by *N.g.* infection at 48 h.p.i. for 12 h. KSHV reactivation as indicated by RFP expression was examined by fluorescence microscopy at 72 and 96 h.p.i. (Figure S3B). With infection at MOI = 5 and 10, all cells were GFP positive and RFP negative, indicating that KSHV infection remains latent. At 72 and 96 h.p.i., no RFP-positive cells were observed in either KSHV or KSHV plus *N.g.* groups (Figure S3C). This finding indicates that *N.g.* fails to reactivate KSHV in HOK cells. Collectively, these results show that *N.g.*, an AIDS-associated bacterial pathogen, is unable to reactivate KSHV but promotes KSHV lytic replication in HOK cells.

2.2 | *N.g.* Induces the Expression of KSHV RTA

KSHV RTA is required to initiate the cascade of viral gene expression [19]. We reasoned that *N.g.* increases RTA expression to promote KSHV lytic replication in the oral cavity. We therefore examine the changes in KSHV transcripts upon bacterial infection, using samples at 18 and 24 h, the early stage of coinfection. As expected, the expression of genes of immediate early (PAN and ORF57) and early (ORF59) phases were increased by approximately 100-fold and sixfold with *N.g.* infection (Figure 3A). The expression of RTA and subsequent RTA-transactivated lytic genes of KSHV was greatly enhanced by *N.g.* infection (Figure 3B). These findings support our hypothesis that *N.g.* infection increases RTA expression to promote KSHV lytic replication.

To determine the effect of *N.g.* infection on RTA-mediated transcription, we performed a reporter assay using constructs containing RTA-responsive elements in HOK cells and 293T cells. Our results show that *N.g.* infection indeed elevated the transcriptional activation of RTA-responsive promoters, including those of RTA,

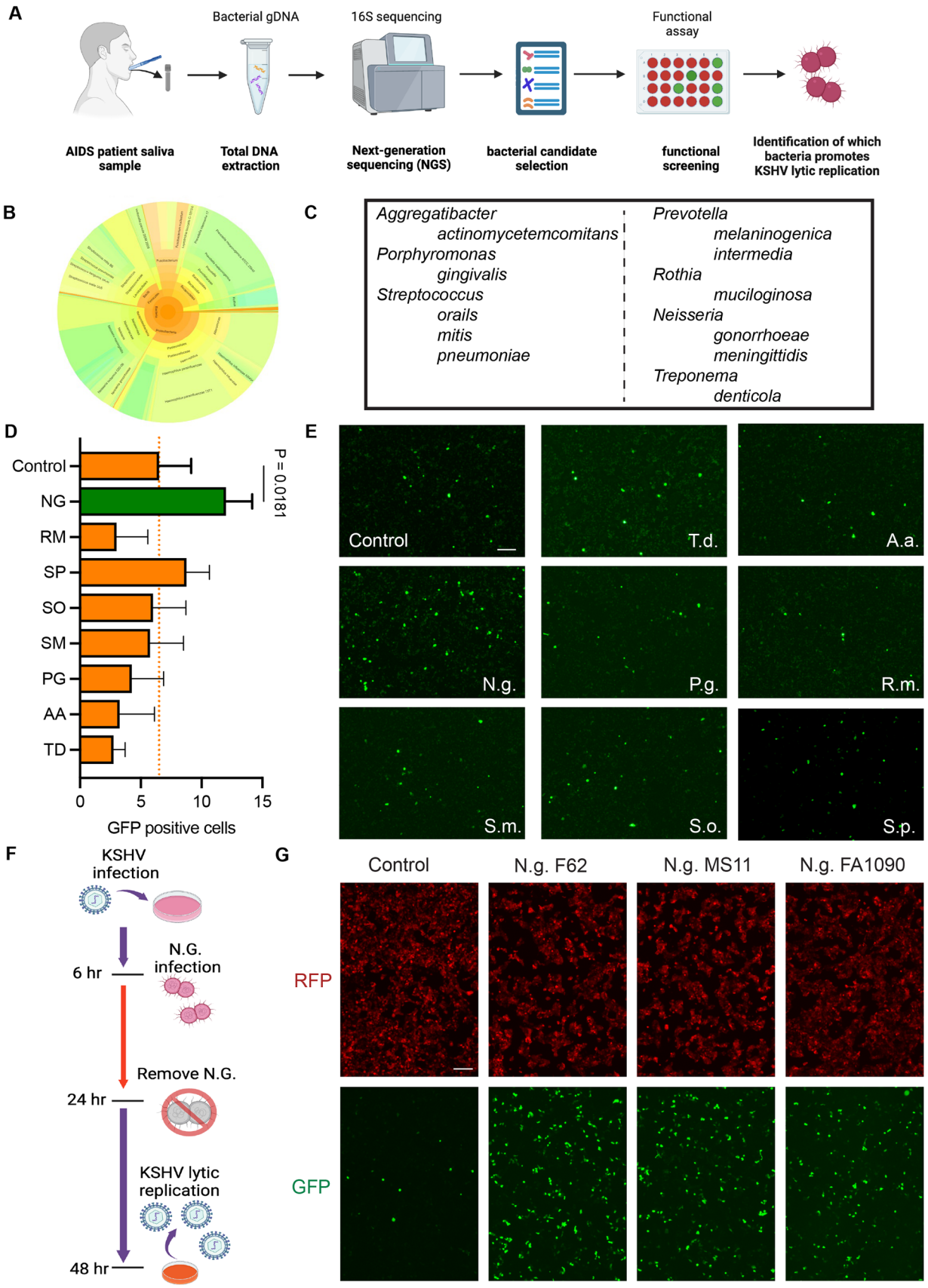

FIGURE 1 | Functional screening of oral bacterial pathogen in promoting KSHV lytic replication. (A) Scheme of screening bacterial pathogen that promotes KSHV lytic replication. (B) Representation of oral bacterial composition via 16S sequencing in saliva samples from AIDS patients. (C) The list of selected bacteria for functional assay of KSHV replication. (D) GFP-positive cell counts of KSHV in HOK cells infected with KSHV and bacteria. (E) Images of HOK cells coinfected with KSHV and oral bacteria. (F) Infection protocol of KSHV and *N.g.* (G) Images of HOK cells infected with KSHV and various *N.g.* strains, including F62, MS11, and FA1090. Statistical significance was calculated using unpaired two-tailed *t*-tests. Data are presented as mean values ± SD.

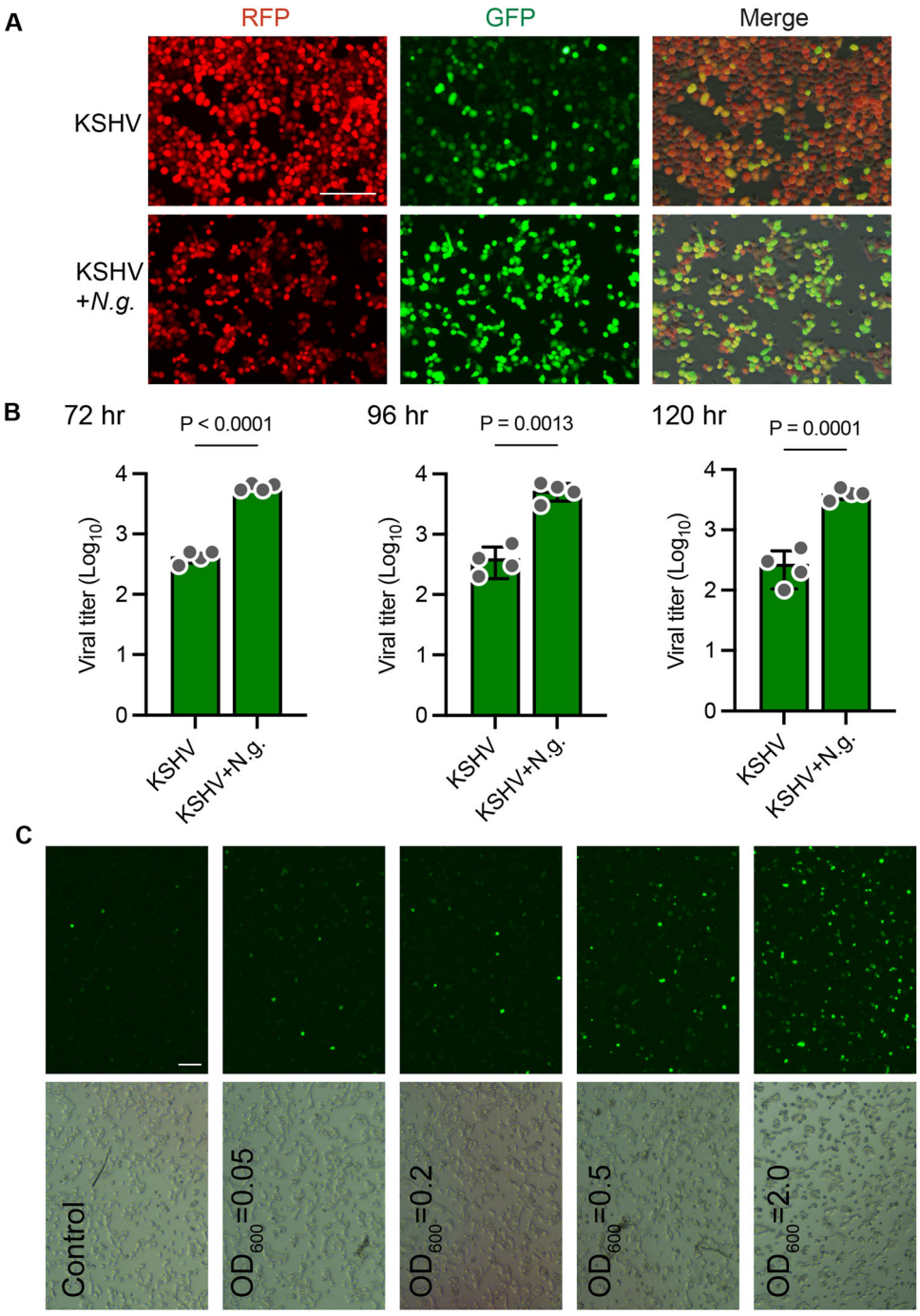

FIGURE 2 | *N.g.* accelerates KSHV lytic replication. (A) Representative images of HOK cells infected with KSHV RGB in the absence and presence of *N.g.* infection. (B) Viral titer of KSHV in coinfected HOK cells at 72, 96, and 120 h.p.i. C. *N.g.* stimulates KSHV replication in a dose-dependent manner. Statistical significance was calculated using unpaired two-tailed *t*-tests. Data are presented as mean values ± SD.

PAN, and ORF57 (Figure 3C). We also performed the experiment to examine whether *N.g.* alone activated the ORF50 promotor in the absence of RTA in transfected HOK cells. However, *N.g.* demonstrated a limited effect on the expression of the ORF50 promoter by a luciferase assay (Figure S3D). Immunoblotting analysis for major viral antigens showed that RTA, K3, and TK (ORF21) were greatly increased by *N.g.* infection, while a modest increase in ORF75 (vGAT) was only obvious at 48 h postinfection (Figure 3D). These results demonstrate that *N.g.* infection can increase KSHV lytic gene expression at the protein level.

Bacteria-triggered host immune response was well studied on Toll-like receptor (TLR) signaling pathways via bacterial-derived structural components, such as lipopolysaccharides. Further, activation of TLRs was found to sufficiently reactivate latent KSHV and increase viral replication [20]. We, therefore, performed an experiment using heat-inactivated *N.g.* to explore the role of bacterial structural components on KSHV lytic replication. Compared with active *N.g.* infection, heat-inactivated *N.g.* had a limited effect on KSHV lytic replication (Figure 4A). Heat-inactivated *N.g.* had marginal or no effect on the

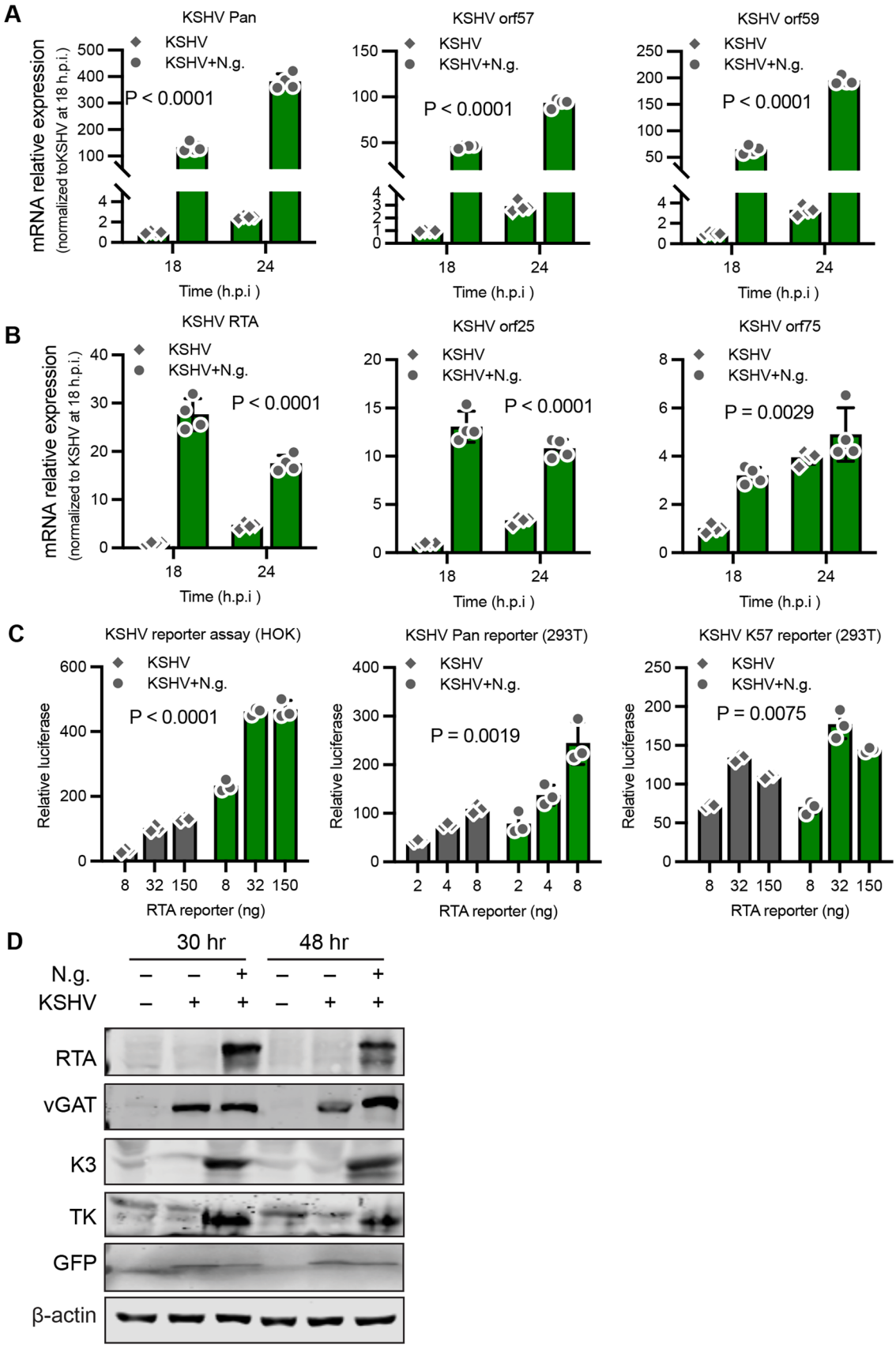

FIGURE 3 | *N.g.* infection upregulates KSHV viral transcription and induces RTA expression. (A) Viral transcripts of immediate early and early genes in infected HOK cells. (B) Viral transcripts of RTA and late genes in infected HOK cells. (C) Reporter assay of RTA in transfected HOK and 293T cells, without KSHV infection. (D) Immunoblot of viral protein expression in mock, KSHV, and KSHV + *N.g.* groups at 30 and 48 h.p.i. Statistical significance was calculated using two-way ANOVA between KSHV and KSHV + *N.g.* Data are presented as mean values ± SD.

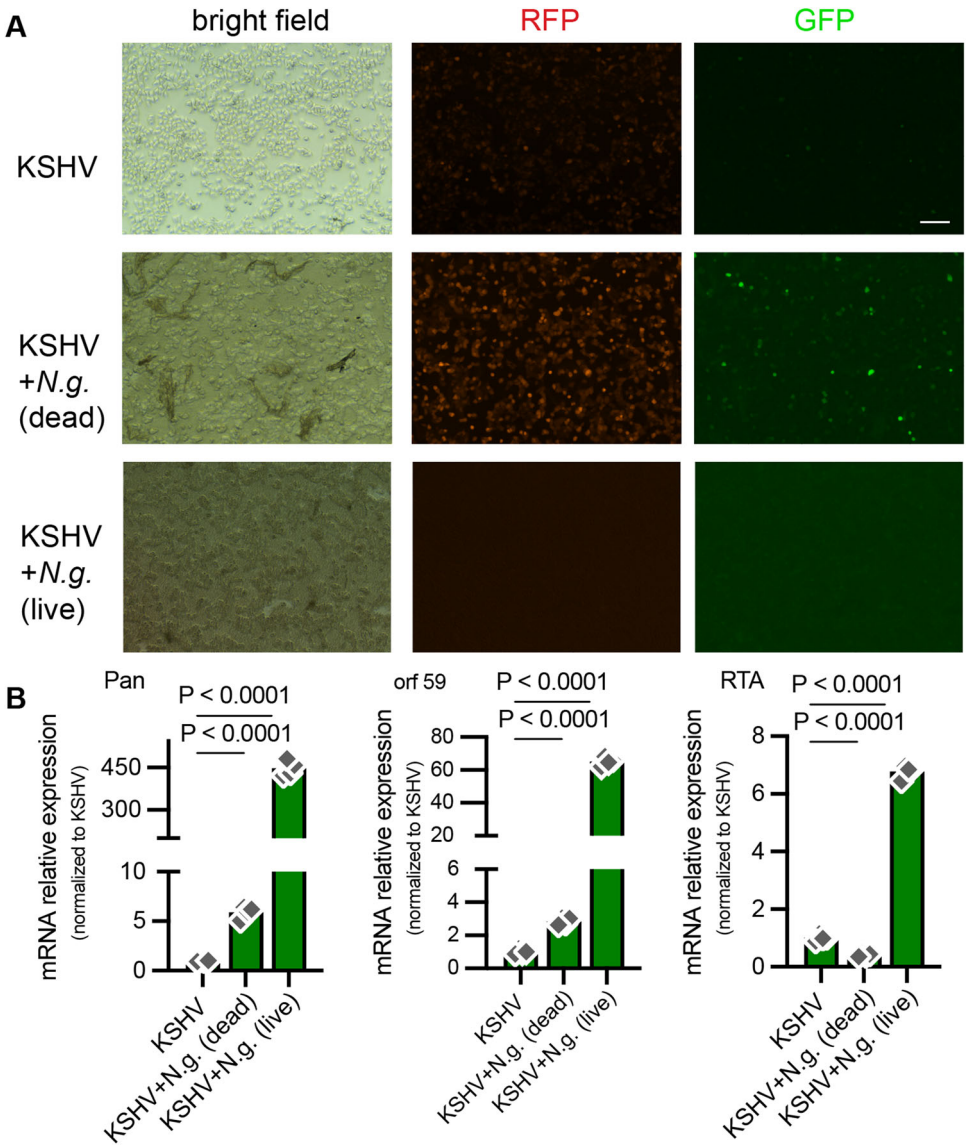

FIGURE 4 | Cellular substances of *N.g.* have limited potential to stimulate KSHV lytic replication. (A) Representative images of infected HOK cells using live and dead bacteria. (B) Viral transcripts in KSHV-infected HOK cells stimulated with live and dead *N.g.*

expression of KSHV lytic genes, for example, PAN and ORF 59 (Figure 4B). Thus, it is unlikely that lipopolysaccharides of *N.g.* or other bacteria-derived metabolites and proteins have significance in enhancing KSHV lytic replication.

2.3 | *N.g.* Promotes MHV68 Replication, But Inhibits HSV-1 Replication

Murine gammaherpesvirus 68 (MHV68) is genetically related to human gammaherpesviruses, that is, KSHV and EBV, and serves as a model for studying in vivo infection of human gammaherpesviruses. We performed a similar coinfection experiment using MHV68-infected HOK cells and examined viral lytic replication by viral titer and viral lytic gene expression. *N.g.* coinfection increased MHV68 replication by ~5-fold (Figure 5A). Consistent with this observation, *N.g.* infection elevated the expression of Orf9, Orf21, and Orf60 by more than 10-fold at MOI = 0.05 and more than 25-fold at MOI = 0.5 (Figure 5B,C). To further probe whether the stimulation is specific to gammaherpesviruses, we examined the impact of *N.g.* infection on HSV-1, a neurotropic alphaherpesvirus. Surprisingly, HSV-1 replication was inhibited by *N.g.* infection (Figure 5E), which correlated with the downregulated expression of the immediate early, early, and late genes by *N.g.* coinfection. These findings indicate that *N.g.* selectively promotes the lytic replication of gammaherpesviruses.

2.4 | *N.g.* Infection Promotes Glycolysis and Nucleotide Synthesis

As shown in Figure 3A,B, *N.g.* coinfection dramatically elevated the expression of KSHV transcripts; thus, we hypothesize that the production of nucleotides, which is the major supply of DNA and RNA synthesis, is accelerated due to *N.g.* coinfection. To profile the metabolites in infected cells, we performed a metabolomic analysis of mock-, KSHV-infected, and KSHV and *N.g.* coinfected HOK cells using liquid chromatography–mass spectrometry. This analysis identified 164 metabolites that were significantly altered among the three groups (Figure 6A).

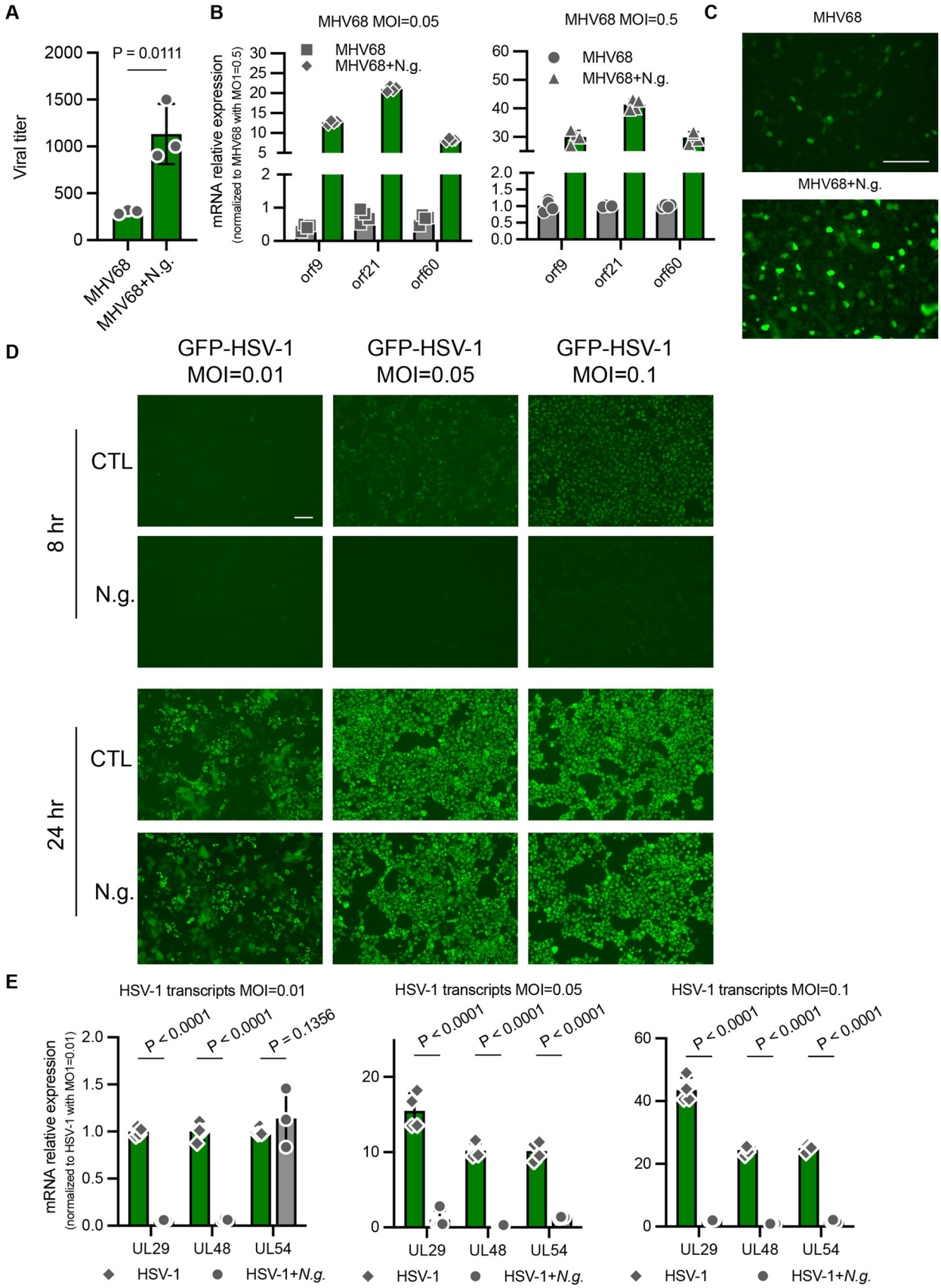

FIGURE 5 | *N.g.* promotes MHV68 replication, but inhibits HSV-1 replication. (A) Viral titer of MHV68 in the supernatant of HOK cells infected with MHV68 with and without *N.g.* (B) Transcripts of MHV68 in the infected HOK cells. (C) Representative images of MHV-68-infected HOK cells. (D) Microscopy of HOK cells infected with HSV-1 and HSV-1 + *N.g.* at 8 and 24 h.p.i. (E) HSV-1 transcripts of immediate early, early, and late genes in infected cells. Statistical significance was calculated using unpaired two-tailed *t*-tests. Data are presented as mean values ± SD.

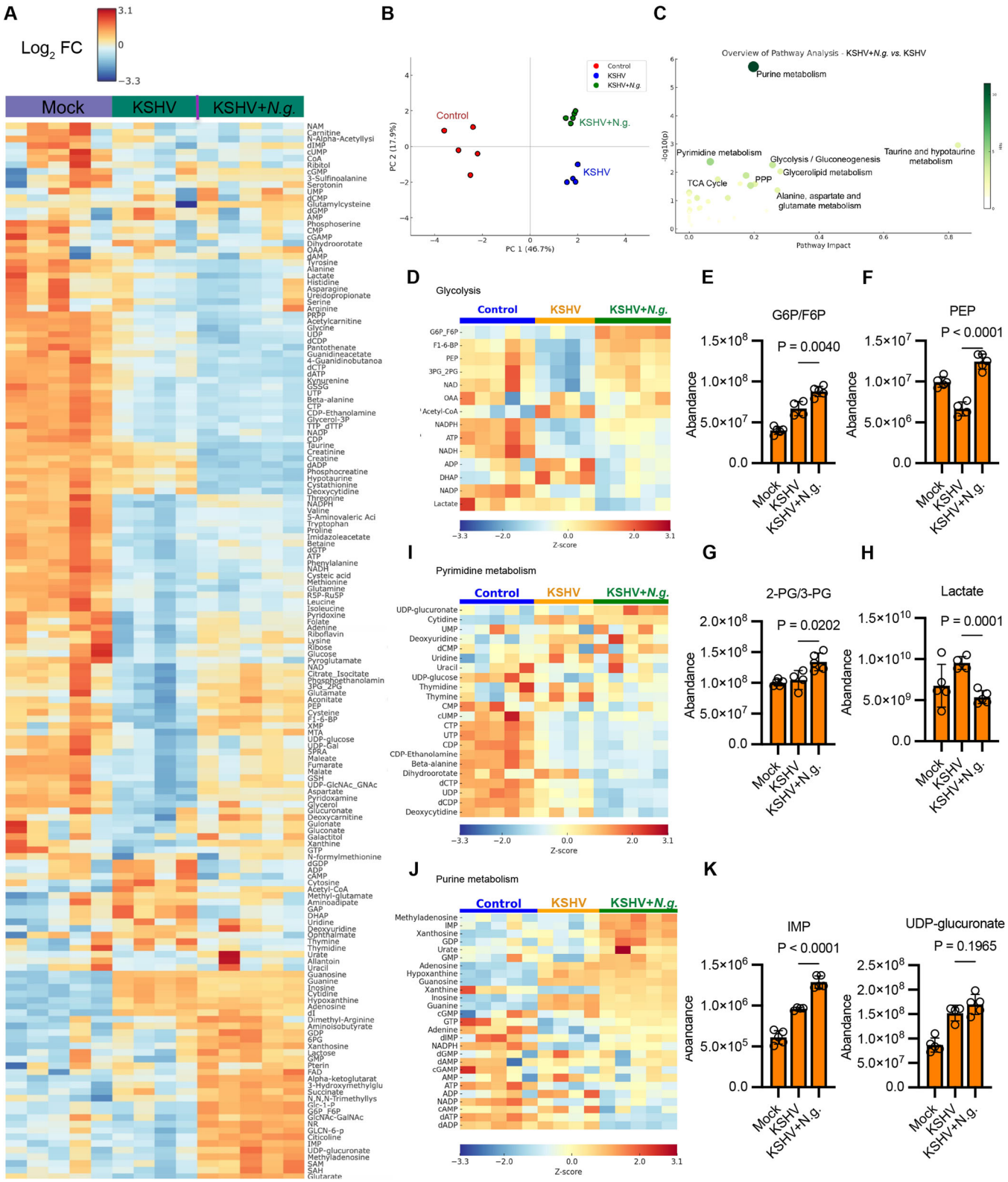

FIGURE 6 | Metabolic reprogramming in HOK cells infected with KSHV and *N.g.* (A) Heatmap of metabolites in HOK-infected cells. For normalization, each biochemical is rescaled to set the median equal to 1. (B) PCA analysis of mock, KSHV, and KSHV + *N.g.* group. (C) Pathway analysis of metabolites in KSHV and KSHV + *N.g.* infected cells. The x-axis represents the degree of change based on the comparison between two groups, with higher values indicating more significant metabolic alternation. The y-axis shows the value of the $-\log_{10}(p \text{ value})$, in which a higher value suggests greater statistical significance. In the plot, each point's size and color intensity reflect the number of hits (metabolites) detected within that pathway. (D) Heatmap of metabolites related to glycolysis. (E–H) MS Abundance of G6P/F6P (E), PEP (F), 2-PG/3-PG (G), and lactate (H) in HOK cells quantified by LC/MS. (I–J) Heatmap of metabolites related to pyrimidine metabolism (I) and purine metabolism (J) in HOK-infected cells. (K) The abundance of IMP and UDP-glucuronate in HOK cells quantified by LC/MS. For normalization in heatmaps, each biochemical is rescaled to set the median equal to 1. Statistical significance was calculated using unpaired two-tailed *t*-tests. Data are presented as mean values ± SD.

Samples were harvested at 30 h.p.i. in which KSHV remains at the early stage of lytic replication, following the same infection protocol as previously described (Figure 1D). The principal component analysis (PCA) plot shows distinct clusters among each experimental sample and the differentiation of each group in the multifactorial dataset. In our metabolomic analysis, we identified three clusters: mock, KSHV, and KSHV + *N.g.*, and the distinct metabolic shift among these groups (Figure 6B). Figure 6C is the pathway analysis between KSHV + *N.g.* versus KSHV to present the major pathway(s) that were significantly influenced by *N.g.* infection, including the glycolysis and purine and pyrimidine metabolism. The x-axis (Pathway Impact) represents the degree of change based on the comparison between these two groups, with higher values indicating more significant metabolic alternation. The y-axis shows the value of the $-\log_{10}(p \text{ value})$, in which a higher value indicates greater statistical significance. In the plot, each point's size and color intensity reflect the number of hits (metabolites) detected within that pathway. For example, more than 10 metabolites in the purine metabolism were detected with a significant change in the KSHV + *N.g.* group compared with the KSHV group, suggesting that *N.g.* infection further promotes purine metabolism that may assist KSHV lytic replication. Moreover, consistent with previous findings, KSHV infection induces aerobic glycolysis, as indicated by increased lactate production (Figure 6A,B) [21, 22]. The major metabolites of glycolysis, such as glucose-6-phosphate/fructose-6-phosphate (G-6-P/F-6-P) and 2-phosphoglyceric acid/3-phosphoglyceric acid (2-PG/3-PG), were slightly elevated in the KSHV-infected cells due to the infection stage but significantly increased in the KSHV and *N.g.* coinfected cells (Figure 6D–G). Other glycolytic intermediates, such as fructose-1,6-biphosphate (F-1,6-BP) and phosphoenolpyruvate (PEP), were also augmented in the KSHV and *N.g.* coinfected cells (Figure 6D,G). These results agree with the ongoing KSHV replication in the infected cells, as we and others observed previously [22, 23]. However, KSHV coinfection with *N.g.* decreased the level of intracellular dihydroxyacetone phosphate (DHAP) and lactate compared to KSHV-infected cells (Figure 6D,H), suggesting the alternative regulation by bacterial stimulation in KSHV infection. In addition to the activation of glycolysis, purine and pyrimidine metabolism and amino acid metabolism represented by alanine/aspartate, glutamate, and taurine/hypotaurine metabolism were further activated by *N.g.* coinfection (Figure 6C,I–K). These findings indicate that *N.g.* regulates cellular metabolism, which synergizes to support KSHV lytic replication.

3 | Discussion

In most infected individuals, KSHV remains in latency and has limited potential to develop cancer. However, in events such as immunosuppression (e.g., HIV infection), inflammation, and coinfection with bacterial pathogens and other viruses, KSHV will reactivate and develop a productive infection that contributes to sarcomagenesis [24]. It is of great importance to identify the physiological factors and the underlying mechanism of KSHV reactivation, which will pave the way for developing antiviral and antitumor therapy against KSHV and its associated diseases such as KS and lymphoma.

As an obligate intracellular pathogen, KSHV depends on the cellular machinery for synthesizing macromolecules to support viral progeny production. Employing metagenomic analysis and functional assays, we identified that *N.g.* is capable of promoting KSHV lytic replication. Mechanistically, *N.g.* infection appears to upregulate RTA expression as well as RTA-mediated gene expression. Metabolic profiling showed that *N.g.* coinfection accentuates the key biosynthesis pathways underpinning KSHV lytic replication. These results highlight a synergism between a bacterial pathogen and an oncogenic virus. In the oral cavity, the abundance of each bacterial genus, species, and stain is distinct and dynamic. However, the local concentration of a relatively low-density bacterial pathogen within a particular infection site, such as a periodontal pocket, may be significantly higher than its sampled oral concentration. Our screening strategy started with an equal concentration of bacteria genera to minimize the test variables, but it could exclude other potential bacterial candidates that may affect KSHV infection at lower or higher concentrations. Re-examining the function of other bacteria with varying concentrations should be considered in future work to further characterize the role of oral bacteria and bacterial community in KSHV replication and reactivation.

Both *N.g.* and KSHV are prominent sexually transmitted agents in the context of HIV infection, signifying their physiological interaction in AIDS-associated malignancies. Besides sexual transmission, kissing, saliva exchange, and oral sex are possible transmission routes for both *N.g.* and KSHV [14, 17]. The presence of viable *N.g.* in the saliva becomes a stimulator for KSHV replication by elevating KSHV viral load in the oral cavity, increasing the risk of KSHV transmission among individuals, particularly in AIDS patients. *N.g.* evolved multiple strategies to adapt to various host conditions during asymptotic and pathogenic infection [13]. Studies on host immune attack and antibiotic resistance of *N.g.* infection were well documented [13]; however, the mechanism of how *N.g.* alters the cellular metabolism remains unclear. By using human promyelocytic HL-60 cells for *N.g.* infection, Britigan et al. reported that *N.g.* competes for oxygen with human neutrophils and consumes lactate released from neutrophils, as the carbon source for its catabolism [25]. Later, three lactate dehydrogenases, D-lactate dehydrogenase (LdhD), L-lactate dehydrogenase (LldD), and NAD^+-dependent D-lactate dehydrogenase were identified [26]. To secure lactate for survival and growth, *N.g.* stimulates aerobic glycolysis but decreases oxidative phosphorylation of infected cells to promote lactate production [27]. In fact, we observed a significant decrease of cellular lactate in the KSHV and *N.g.* coinfected cells, suggesting the consumption of lactate by *N.g.* (Figure 6H). The *N.g.*-mediated removal of lactate may positively influence KSHV lytic replication via further fueling aerobic glycolysis. While KSHV is an intracellular pathogen and directly acquires metabolites from cell machinery, the induction of aerobic glycolysis and related metabolites by *N.g.* stimulation provides extra materials such as energy and nucleotides inside the infected cell for KSHV lytic replication. Future work on dissecting which bacterial component(s) regulate the metabolic enzymes and metabolite transporters in the host cells and how they interact with the viral factors will advance the understanding of this pathogenetic collaboration on KSHV reactivation.

Our work presents the potent inductive effect of *N.g.* on KSHV lytic replication and pinpoints the crosstalk between bacteria and virus-interfered cellular events. Most importantly, findings from this study advance our understanding of polymicrobial interaction and explore a framework for microbial pathogenesis research.

4 | Materials and Methods

4.1 | Human Saliva Sample Collection

Patients first rinsed with mouthwash, and saliva was collected in a wide-mouth 50 mL Nalgene tube. A total of 3–5 mL of mouthwash is generally applied. The patients were requested not to eat or smoke before sample collection. The samples were transferred to round bottom, screw-cap 1.5 mL tubes, in 1 mL aliquots, and centrifuged at 17 000 g for 5 min. The pellet was resuspended in 200 μL PBS for DNA extraction using QIAamp DNA Mini-kit (Qiagen), and extracted samples were stored at −80°C for further examination.

4.2 | Cell Culture and Virus Production

HOK cells were provided by Dr. Ren Sun (University of California, Los Angeles) and cultured in Keratinocyte Basal Medium (KBM) (Lonza, CC-3101) supplemented with KBM SingleQuots Supplements and Growth Factors (Lonza, CC-4131) and maintained in the humidified incubator with 5% CO_2 at 37°C. iSLK 219, iSLK RGB, and BAC16 cells were cultured in DMEM medium containing 10% FBS, 1% penicillin–streptomycin, 10 μg/mL puromycin, 250 μg/mL G418, and 400 μg/mL hygromycin. To reactivate KSHV, 60% confluent cells were maintained in the DMEM with 10% FBS, 1% penicillin–streptomycin, 1 μg/mL doxycycline, and 1 mM sodium butyrate. At 48 h.p.i., the KSHV-containing medium was harvested and passed through a 0.45 μm PES filter, followed by concentrating at 8000 rpm, 4°C, for 15 min to remove cell debris. KSHV virions were pelleted by ultrahigh-speed centrifugation at 32 000 rpm (Beckman rotor Type 45i), 4°C, for 90 min. The viral pellet was washed with PBS and resuspended in KBM medium at 4°C overnight. Viral stock was aliquoted and stored at −80°C for further use.

To titrate KSHV from concentrated stock and infected cells, each virus-containing suspension and supernatant was subject to a series of 10-fold dilutions. Diluted samples were used to infect 293T cells in 12-well plates, as described previously [28]. At 48 h.p.i., RFP- (rKSHV RGB) or GFP-positive (rKSHV219 and BAC16) cells were counted with a fluorescence microscope. The well containing the least number of fluorescent cells will be used for titer quantification: number of fluorescent cells × dilution factor.

4.3 | Bacterial Growth

N.g. strains were gifted by Dr. Douglas T Golenbock (UMass Chan Medical School). For cultivation, the *N.g.* glycerol stock was plated on the chocolate agar medium (Thermo Scientific) with sterile cotton sticks for 1–2 days in the humidified incubator with 5% CO_2 at 37°C (please see the left image). For infection, bacterial colonies were harvested from the plate, resuspended in a KBM medium, and homogenized via vortexing. OD600 was determined using Nanodrop (Thermo). KSHV-infected HOK cells were incubated with *N.g.*-containing KBM medium for a designated time. OD600 1.0 equals 3.6×10^8 cfu [29, 30].

4.4 | KSHV and *N.g* Coinfection

Before KSHV infection, one well of HOK cells was sacrificed for cell counting with trypan blue staining. The amount of virus used for infection with MOI = 30 was calculated as 30 × cell numbers. For coinfection, HOK cells were first infected with high-titer KSHV (MOI = 30, RGB-BAC16 KSHV expresses RFP and GFP as indicators for infection and lytic replication, respectively [31]) with centrifugation infection and stimulated with *N.g* (OD600 = 1.0) after 6 p.i.h. for an additional 18 h, by replacing *N.g.*-contained KGM. At the designated postinfection time, the supernatant was collected for viral titration, and infected cells were harvested for the analysis of viral transcription activity, viral protein expression, and metabolomics.

4.5 | DNA and RNA Extraction and RT-PCR

Total DNA was extracted using Quick-DNA Midiprep Plus Kit (Zymo Research) following the manufacturer's instructions. Total RNA was extracted using TRIzol reagent (Invitrogen) following the manufacturer's protocol. DNase I was used to eliminate the contamination of genomic DNA. Each reverse transcription reaction (20 μ) includes a total of 1 μg RNA as a template, oligo dT (2 μM), dNTP (0.5 mM), 5× transcription buffer, and M-MLV reverse transcriptase (Promega, M1701). In the quantitative real-time PCR (qRT-PCR) reaction, the cDNA template, corresponding primer set (Table S1), and SYBR master mix (Applied Biosystems) were assembled. Cycle conditions were as follows: 95°C for 10 min and 95°C for 15 s followed by 55°C for 1 min (40 cycles). Fold change of mRNA expression for each target gene was calculated using the $2^{-\Delta\Delta Ct}$ method, normalized to the human housekeeping gene ACTB.

4.6 | Immunoblotting

Cells were pelleted and solubilized in lysis buffer (50 mM Tris-HCl, pH 7.4, 1 mM EDTA, 150 mM NaCl, 0.25% Na-deoxycholate, 1% NP-40, 0.10% SDS, and 1% TritonX-100 on ice for 30 min). Cell lysates were centrifuged at 12 000 rpm at 4°C for 10 min, and the soluble fraction was denatured in loading buffer at 95°C for 10 min. Proteins were separated by SDS-PAGE and subsequently transferred to nitrocellulose membranes for antibody incubation. Membranes were blocked with 5% skim milk and probed with primary antibodies overnight at 4°C, later incubated with secondary antibodies (IRDye800-conjugated 1:10 000 dilutions, LI-COR Biosciences) for 1 h before exposure on the LI-COR Odyssey infrared imager. Images were processed using Image Studio Version 4.0 (LI-COR Biosciences).

Primary antibodies (diluted 1:1000) were used in this study: KSHV RTA (ORF50), ORF75 (vGAT), and ORF21 (kTK) polyclonal antibodies were produced by Cocalico Biologicals (Reamstown, Pennsylvania) following standard protocols. The anti-GFP (sc-9996) was purchased from Santa Cruz, and the anti-b-actin (MA1-140, mouse monoclonal) from Invitrogen.

4.7 | Luciferase Reporter Assay

HOK and 293T cells seeded in 12-well plates were transfected with the PAN promoter reporter cocktail (100 ng) with varying doses of RTA plasmids (0, 8, 32, and 150 ng). *N.g.* infection was performed at 24 h, and cells were harvested at 48 h by trypsinization. Cell pellets were further lysed with lysis buffer (Promega) for 30 min at room temperature. Luciferase activity was determined by a microplate reader (FLUOstar Omega) using cell-free whole-cell lysates. β-Galactosidase was included as an internal control.

4.8 | Microscopy

At the designated time point, live cells were imaged via a Nikon TI2-D-PD (599378) microscope. All images were processed with NIS-Elements version 5.11.

4.9 | Mass Spectrometry

For metabolite analysis, mock-, KSHV-, and KSHV + *N.g.* infected HOK cells (approximately 2×10^6) were washed with PBS and ice-cold 150 mM ammonium acetate (NH4AcO, pH 7.3) at the designated time point. The cold 80% (v/v) methanol (1 mL), pre-chilled at −80°C, was added to each 6-well for metabolite extraction, followed by incubation at −80°C for 20 min. Cells were scraped off after incubation and pelleted at 4°C for 10 min at 21 000 g. The supernatant was transferred into a new centrifuge tube and vacuum-dried at room temperature. The dried pellet was re-suspended in the HPLC grade ultrapure water and analyzed on a Q-Exactive Plus hybrid quadrupole-Orbitrap MS coupled with Vanquish UHPLC system (ThermoFisher Scientific) in polarity switching mode (+3.00 kV/−2.25 kV) with an m/z window ranging from 65 to 975. Mobile phase A: 5 mM NH4AcO, pH 9.9, and mobile phase B: acetonitrile. Metabolites were separated on a Luna 3 µm NH2 100 NH2 100 Å (150 × 2.0 mm) column (Phenomenex), with a flow rate of 0.3 mL/min, gradient from 15% A to 95% A in 18 min, followed by an isocratic step for 9 min and re-equilibration for 7 min. Based on retention time and standard compound (Sigma), each metabolite was identified and quantified by peak area integration using TraceFinder 4.1 (ThermoFisher Scientific). The heatmap, PCA analysis, and pathway analysis were performed using MetaboAnalyst, a web-based platform for statistical, functional, and pathway analysis of metabolomics data [32]. Plots were made with MetaboAnalyst and R programming.

4.10 | Statistical Analysis

Data represent the mean of three independent experiments, and error bars denote SD unless specified otherwise. Statistical analysis was performed with GraphPad Prism 10 for unpaired two-tailed *t*-test and two-way ANOVA. A p value less than 0.05 is considered statistically significant.

Author Contributions

Shu Feng and Pinghui Feng conceived the study. Shu Feng conducted the experiments and analyzed the data. Wen Fu performed the metabolomics analysis. Shutong Li and Wayne Yeh assisted with KSHV production and microscopy. Pinghui Feng and Casey Chen supervised the project. Pinghui Feng and Charles Brenner secured funding support. Shu Feng and Pinghui Feng wrote the manuscript with comments collected from all authors.

Acknowledgments

We are grateful to Dr. Zhiqiang Qin (University of Arkansas) for sharing the patient saliva samples with us and Dr. Douglas T Golenbock (UMass Chan Medical School) for providing *N.g.* strains. We thank Dr. Hui Wu, Dr. Ashu Sharma, and Dr. Malcolm E. Winkler for gifting bacterial strains included in this study. We also appreciated the assistance provided by Drs Wenjie Zhu, Yongzhen Liu, Jiang Zhong, and Yuzheng Zhou in this study. This study is supported by a startup fund from the Herman Ostrow School of Dentistry of USC and awards from NIH (CA185192 and AG070904 to Pinghui Feng).

Conflicts of Interest

C.B. is a chief scientific advisor of ChromaDex and co-founder of Alphina Therapeutics. All other authors declare no Conflict of Interest.

Data Availability Statement

The data that support the findings of this study are available from the corresponding author upon reasonable request.

References

1. Y. Chang, E. Cesarman, M. S. Pessin, et al., "Identification of Herpesvirus-Like DNA Sequences In AIDS-Sssociated Kaposi's Sarcoma," *Science* 266 (1994): 1865–1869, https://doi.org/10.1126/science.7997879.

2. K. W. Wen and B. Damania, "Kaposi Sarcoma-Associated Herpesvirus (KSHV): Molecular Biology and Oncogenesis," *Cancer Letters* 289 (2010): 140–150, https://doi.org/10.1016/j.canlet.2009.07.004.

3. J. Chen, K. Ueda, S. Sakakibara, et al., "Activation of Latent Kaposi's Sarcoma-Associated Herpesvirus by Demethylation of the Promoter of the Lytic Transactivator," *Proceedings of the National Academy of Sciences* 98 (2001): 4119–4124, https://doi.org/10.1073/pnas.051004198.

4. K. K. Aneja and Y. Yuan, "Reactivation and Lytic Replication of Kaposi's Sarcoma-Associated Herpesvirus: An Update," *Frontiers in Microbiology* 8 (2017): 613, https://doi.org/10.3389/fmicb.2017.00613.

5. L. Dai, J. Qiao, J. Yin, et al., "Kaposi Sarcoma–Associated Herpesvirus and *Staphylococcus aureus* Coinfection in Oral Cavities of HIV-Positive Patients: A Unique Niche for Oncogenic Virus Lytic Reactivation," *Journal of Infectious Diseases* (2019): 1331–1341, https://doi.org/10.1093/infdis/jiz249.

6. L. Dai, L. Barrett, K. Plaisance-Bonstaff, S. R. Post, and Z. Qin, "*Porphyromonas gingivalis* Coinfects With KSHV in Oral Cavities of HIV+ Patients and Induces Viral Lytic Reactivation," *Journal of Medical Virology* 92 (2020): 3862–3867, https://doi.org/10.1002/jmv.26028.

7. A. Markazi, W. Meng, P. M. Bracci, M. S. McGrath, and S. J. Gao, "The Role of Bacteria in KSHV Infection and KSHV-Induced Cancers," *Cancers* 13 (2021): 4269, https://doi.org/10.3390/cancers13174269.

8. A. Contreras, H. Nowzari, and J. Slots, "Herpesviruses in Periodontal Pocket and Gingival Tissue Specimens," *Oral Microbiology and Immunology* 15 (2000): 15–18, https://doi.org/10.1034/j.1399-302x.2000.150103.x.

9. A. R. Naqvi, J. Shango, A. Seal, D. Shukla, and S. Nares, "Herpesviruses and MicroRNAs: New Pathogenesis Factors in Oral Infection and Disease?," *Frontiers in Immunology* 9 (2018): 2099, https://doi.org/10.3389/fimmu.2018.02099.

10. J. Webster-Cyriaque, K. Duus, C. Cooper, and M. Duncan, "Oral EBV and KSHV Infection in HIV," *Advances in Dental Research* 19 (2006): 91–95, https://doi.org/10.1177/154407370601900118.

11. A. Markazi, P. M. Bracci, M. McGrath, and S. J. Gao, "*Pseudomonas aeruginosa* Stimulates Inflammation and Enhances Kaposi's Sarcoma Herpesvirus-Induced Cell Proliferation and Cellular Transformation Through Both Lipopolysaccharide and Flagellin," *mBio* 11 (2020): e02843-20, https://doi.org/10.1128/mBio.02843-20.

12. X. Yu, A. M. Shahir, J. Sha, et al., "Short-Chain Fatty Acids From Periodontal Pathogens Suppress Histone Deacetylases, EZH2, and SUV39H1 to Promote Kaposi's Sarcoma-Associated Herpesvirus Replication," *Journal of Virology* 88 (2014): 4466–4479, https://doi.org/10.1128/JVI.03326-13.

13. S. J. Quillin and H. S. Seifert, "*Neisseria gonorrhoeae* Host Adaptation and Pathogenesis," *Nature Reviews Microbiology* 16 (2018): 226–240, https://doi.org/10.1038/nrmicro.2017.169.

14. E. W. Hook, 3rd and K. Bernstein, "Kissing, Saliva Exchange, and Transmission of *Neisseria gonorrhoeae*," *Lancet Infectious Diseases* 19 (2019): e367–e369, https://doi.org/10.1016/S1473-3099(19)30306-8.

15. S. Ramos da Silva and D. Elgui de Oliveira, "HIV, EBV and KSHV: Viral Cooperation in the Pathogenesis of Human Malignancies," *Cancer Letters* 305 (2011): 175–185, https://doi.org/10.1016/j.canlet.2011.02.007.

16. M. He, et al., "Molecular Biology of KSHV in Relation to HIV/AIDS-Associated Oncogenesis," *Cancer Treatment and Research* 177 (2019): 23–62, https://doi.org/10.1007/978-3-030-03502-0_2.

17. V. Minhas and C. Wood, "Epidemiology and Transmission of Kaposi's Sarcoma-Associated Herpesvirus," *Viruses* 6 (2014): 4178–4194, https://doi.org/10.3390/v6114178.

18. F. Cerimele, F. Curreli, S. Ely, A. E. Friedman-Kien, E. Cesarman, and O. Flore, "Kaposi's Sarcoma-Associated Herpesvirus Can Productively Infect Primary Human Keratinocytes and Alter Their Growth Properties," *Journal of Virology* 75 (2001): 2435–2443, https://doi.org/10.1128/jvi.75.5.2435-2443.2001.

19. J. Guito and D. M. Lukac, "KSHV Rta Promoter Specification and Viral Reactivation," *Frontiers in Microbiology* 3 (2012): 30, https://doi.org/10.3389/fmicb.2012.00030.

20. S. M. Gregory, J. A. West, P. J. Dillon, C. Hilscher, D. P. Dittmer, and B. Damania, "Toll-Like Receptor Signaling Controls Reactivation of KSHV From Latency," *Proceedings of the National Academy of Sciences* 106 (2009): 11725–11730, https://doi.org/10.1073/pnas.0905316106.

21. T. Delgado, P. A. Carroll, A. S. Punjabi, D. Margineantu, D. M. Hockenbery, and M. Lagunoff, "Induction of the Warburg Effect by Kaposi's Sarcoma Herpesvirus is Required for the Maintenance of Latently Infected Endothelial Cells," *Proceedings of the National Academy of Sciences* 107 (2010): 10696–10701, https://doi.org/10.1073/pnas.1004882107.

22. Q. Wan, L. Tavakoli, T. Y. Wang, et al., "Hijacking of Nucleotide Biosynthesis and Deamidation-Mediated Glycolysis by an Oncogenic Herpesvirus," *Nature Communications* 15 (2024): 1442, https://doi.org/10.1038/s41467-024-45852-5.

23. T. Delgado, E. L. Sanchez, R. Camarda, and M. Lagunoff, "Global Metabolic Profiling of Infection by an Oncogenic Virus: KSHV Induces and Requires Lipogenesis for Survival of Latent Infection," *PLoS Pathogens* 8 (2012): e1002866, https://doi.org/10.1371/journal.ppat.1002866.

24. R. Thiruvengadam and J. H. Kim, "Therapeutic Strategy for Oncovirus-Mediated Oral Cancer: A Comprehensive Review," *Biomedicine & Pharmacotherapy* 165 (2023): 115035, https://doi.org/10.1016/j.biopha.2023.115035.

25. B. E. Britigan, D. Klapper, T. Svendsen, and M. S. Cohen, "Phagocyte-Derived Lactate Stimulates Oxygen Consumption by *Neisseria gonorrhoeae*. An Unrecognized Aspect of the Oxygen Metabolism of Phagocytosis," *Journal of Clinical Investigation* 81 (1988): 318–324, https://doi.org/10.1172/JCI113323.

26. J. M. Atack, I. Ibranovic, C. L. Y. Ong, et al., "A Role for Lactate Dehydrogenases in the Survival of *Neisseria gonorrhoeae* in Human Polymorphonuclear Leukocytes and Cervical Epithelial Cells," *Journal of Infectious Diseases* 210 (2014): 1311–1318, https://doi.org/10.1093/infdis/jiu230.

27. L. R. Green, J. Cole, E. F. D. Parga, and J. G. Shaw, "*Neisseria gonorrhoeae* Physiology and Pathogenesis," *Advances in Microbial Physiology* 80 (2022): 35–83, https://doi.org/10.1016/bs.ampbs.2022.01.002.

28. S. J. Gao, J. H. Deng, and F. C. Zhou, "Productive Lytic Replication of a Recombinant Kaposi's Sarcoma-Associated Herpesvirus in Efficient Primary Infection of Primary Human Endothelial Cells," *Journal of Virology* 77 (2003): 9738–9749, https://doi.org/10.1128/jvi.77.18.9738-9749.2003.

29. T. Elmros, G. Sandström, and L. Burman, "Autolysis of *Neisseria gonorrhoeae*. Relation Between Mechanical Stability and Viability," *British Journal of Venereal Diseases* 52 (1976): 246–249, https://doi.org/10.1136/sti.52.4.246.

30. M. Takei, Y. Yamaguchi, H. Fukuda, M. Yasuda, and T. Deguchi, "Cultivation of *Neisseria gonorrhoeae* in Liquid Media and Determination of Its In Vitro Susceptibilities to Quinolones," *Journal of Clinical Microbiology* 43 (2005): 4321–4327, https://doi.org/10.1128/JCM.43.9.4321-4327.2005.

31. K. F. Brulois, H. Chang, A. S. Y. Lee, et al., "Construction and Manipulation of a New Kaposi's Sarcoma-Associated Herpesvirus Bacterial Artificial Chromosome Clone," *Journal of Virology* 86 (2012): 9708–9720, https://doi.org/10.1128/JVI.01019-12.

32. Z. Pang, Y. Lu, G. Zhou, et al., "MetaboAnalyst 6.0: Towards a Unified Platform for Metabolomics Data Processing, Analysis and Interpretation," *Nucleic Acids Research* 52 (2024): W398–W406, https://doi.org/10.1093/nar/gkae253.

Supporting Information

Additional supporting information can be found online in the Supporting Information section.